Paper N °3763

Registration Code: S-L1464719232

Evaluation of Ground Motion Selection and Modification Methods on Reinforced Concrete Highway Bridges

X. Liang[1], K. M. Mosalam[2]

[1] *Postdoctoral Researcher, University of California, Berkeley, benliangxiao@berkeley.edu*

[2] *Taisei Professor of Civil Engineering and Director of PEER, University of California, Berkeley, mosalam@berkeley.edu*

Abstract

Reinforced concrete (RC) highway bridges are primary lifeline infrastructures, especially where earthquakes commonly occur. Accurate seismic structural analysis is essential to ensure the safety of bridges. The nonlinear seismic behavior of bridge structures generally exhibits distinct difference in the longitudinal and transverse directions, and thus is sensitive to the selection and modification of the input ground motion records. Performance-based earthquake engineering (PBEE) methodology explicitly takes into account uncertainties in hazard, structural response, damage, and loss estimation. Therefore, PBEE enables a comprehensive understanding of the structural performance in a probabilistic manner. For a given large earthquake scenario, this study takes advantage of the PBEE methodology to develop a reference benchmark probability distribution of seismic demands (*PDSD*) for a given bridge structure considering different intercept angles of the input ground motions. The accuracy and reliability of all *PDSD* estimates from various ground motion selection and modification (GMSM) procedures are evaluated against this reference benchmark *PDSD*. Such evaluation is conducted for several engineering demand parameters (*EDP*s) of three representative RC highway bridges.

Keywords: Benchmark; Engineering Demand Parameter; Ground Motion Selection and Modification; Performance-based Earthquake Engineering; Reinforced Concrete Bridges.

1. Introduction

In urban societies, reinforced concrete (RC) highway bridges play a significant role in transportation and distribution of goods and commuting people. Therefore, they are expected to sustain minor damage and maintain their functionality in the aftermath of earthquakes, which commonly occur in California due to many active faults. In the last two decades, however, even bridges designed according to modern codes were observed to experience poor performance or even collapse during earthquakes caused by inherent vulnerability of the bridge structural systems [1]. Thus, accurate seismic structural analysis of existing and newly designed RC highway bridges is fundamental to estimate their seismic demands [2]. Attributed to continuous improvement of computational power [3], nonlinear time history analysis (NTHA) method as the most suitable approach is becoming increasingly prevalent for analyzing large and complex structures. The intricate nonlinear response of bridges is highly sensitive to the ground motion selection and modification (GMSM) of the input records. Therefore, the GMSM of the input records is a vital prerequisite for accurate seismic analysis.

The GMSM procedures determine the necessary input ground motion (GM) records for the simulations of structures using NTHA. Numerous research efforts focused on developing different GMSM procedures, which are generally categorized into two approaches: (1) amplitude scaling (e.g., [4-6]), and (2) spectrum shape matching procedures (e.g., [7, 8]). A comprehensive review of various GMSM procedures is given in [9, 10]. Although many GMSM procedures are available, there is no consensus regarding a single accurate method and many studies focused on evaluating these procedures. For example, [10-12] compared different GMSM procedures in predicting median responses of seismic demands against developed reference benchmarks. The evaluation studies in the literature were primarily for building structures and considered unidirectional input ground motions. In general, bridge structures exhibit distinct behaviors in the longitudinal and transverse directions. Hence, bidirectional GM studies focused on highway bridges are conducted in this study.

The objective of this study is to evaluate several popular GMSM procedures in predicting the probability distributions of seismic demands (*PDSD*) of RC highway bridges with nonlinear response due to large earthquakes. Therefore, all conducted analyses in this paper are based on a selected large earthquake scenario. In order to effectively evaluate the GMSM procedures, a reference benchmark *PDSD* should be established. A framework of performance-based earthquake engineering (PBEE) was developed at the Pacific Earthquake Engineering Research (PEER) Center, which explicitly takes into account uncertainties in earthquake hazard, structural response, damage and loss estimation [13]. PEER PBEE enables comprehensive understanding of the structural performance in a probabilistic manner. In the context of a given large earthquake scenario, this study takes advantage of the PEER PBEE to develop the reference benchmark *PDSD* for the investigated bridge structures considering different intercept angles of the input GMs. The intercept angle is defined herein as the angle between the Fault-Normal direction (strike-normal GM component) and the longitudinal direction of the bridge structure [14]. The accuracy and reliability of all *PDSD* estimates from the investigated GMSM procedures are then evaluated against this reference benchmark *PDSD*. Such evaluations are conducted on several selected engineering demand parameters (*EDP*s) for three representative RC highway bridges, designated as bridges A, B, and C in this study.

2. Bridge Structures and Analytical Models

Three representative RC highway bridge structures are used for evaluating the GMSM procedures. The selected bridges, designed after 2000 with characteristics and configuration summarized in Table 1, reflect common bridge engineering practice in California. Extensive analytical modeling and simulations for these three bridges can be found in [15]. The software OpenSees [16] is used for the simulations where the models explicitly include seat-type abutments, shear keys, expansion joints, column-bents, and superstructure. The adopted modeling is briefly described in the following paragraphs and a detailed explanation of the modeling assumptions can be found in [14].

The bridge superstructure that consists of the bridge deck and the cap-beam is modeled as elastic beam-column elements with uncracked section properties. The bridge columns are modeled by nonlinear force-based beam-column elements with fiber-discretized cross-sections and 10 integration points along the column height.

Three constitutive models are utilized simultaneously in a fiber discretized cross-section: (1) confined concrete for the core, (2) unconfined concrete for the cover, and (3) steel for the reinforcing bars. In OpenSees, *Concrete01* and *Steel02* models are used for concrete and reinforcement, respectively.

Table 1. Characteristics of the selected bridges.

Bridge	A	B	C
Name	Jack Tone Road Overcrossing	La Veta Avenue Overcrossing	Jack Tone Road Overhead
Number of spans	2	2	3
Column bent	Single-column	Two-column	Three-column
Column radius	33.1 in.	33.5 in.	33.1 in.
Column height	22.0 ft.	22.0 ft.	24.6 ft.
Fundamental period	0.7 sec	1.1 sec	1.6 sec
Configuration	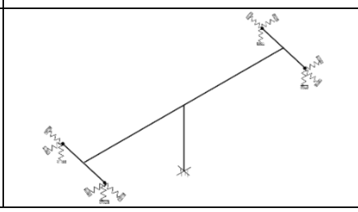	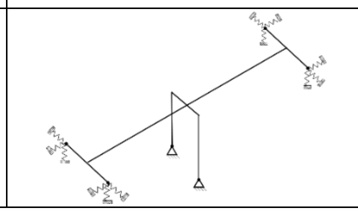	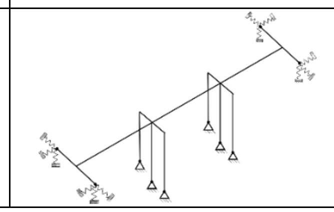

Two modeling approaches, namely Type I and Type II, are considered for the abutment (Figure 1). Both approaches explicitly take into account the longitudinal response of the backfill and expansion joint, the transverse response of the shear keys, and the vertical response of the bearing pads and the stemwall. In Type I (Figure 1a), two nonlinear springs, one at each end, connected in series to gap elements, are used to model the passive backfill response and the expansion joint, respectively [17]. The shear key response is modeled using an elastic-perfectly-plastic backbone. Vertical response of the bearing pads and stemwall is modeled by two parallel springs, one at each end (note that only one side is labelled in Figure 1), to represent the stiffness values. In Type II (Figure 1b), the number of nonlinear springs connected in series to the gap elements is increased to five and the shear key response is modeled using a nonlinear spring with a tri-linear backbone.

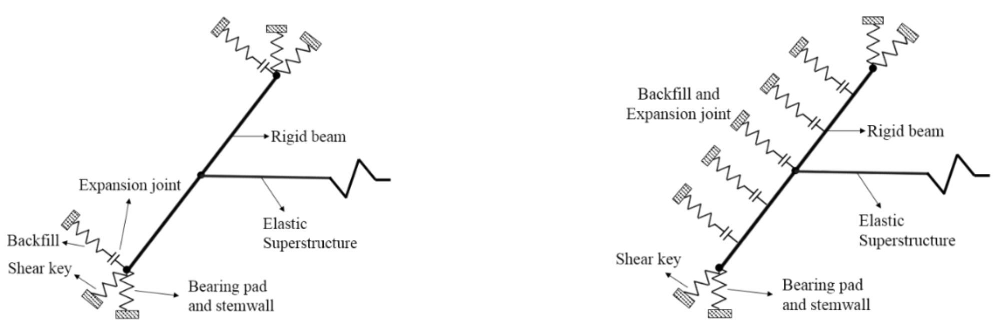

a) Type I b) Type II

Figure 1. Abutment modeling with springs and gap elements.

3. Earthquake Scenario

The evaluation of the *PDSD* estimates from the investigated GMSM procedures against the reference benchmark *PDSD* in this study is based on a selected large earthquake scenario summarized as follows:

***M7 Scenario**: A magnitude* 7.0 *earthquake event occurring on a strike-slip fault, at a site that is 10 km from the fault rupture on a soil with* $V_{s,30}$ *(shear wave velocity for the top 30 m of the soil profile) based on the bridge soil profile* [18]. *The target spectrum for this scenario is selected as the one with* 1.5 *standard deviation above* ($+1.5\varepsilon$) *the median spectrum using the attenuation model in* [19].

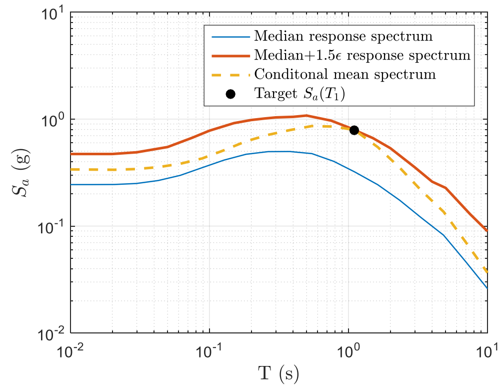

Figure 2. Response spectra for the selected earthquake scenario of bridge B site.

Figure 2 shows the median and $+1.5\varepsilon$ spectra associated with this scenario from the selected attenuation model [19]. Also shown in Figure 2 is the conditional mean spectrum (*CMS*) [8] anchored at the fundamental period of bridge B, i.e., 1.1 sec.

4. Benchmark Probability Distribution of Seismic Demands

The PEER PBEE methodology aims to robustly divide the performance assessment and design process into logical stages that can be studied and resolved in a systematic and consistent manner [20]. These stages of the process contain the definition, description, and quantification of earthquake intensity measure, structural response, damage, and loss. Accordingly, uncertainties in these stages can be explicitly taken into account [13], which enable comprehensive understanding of the structural performance in a probabilistic manner. The well-known PEER PBEE formula originally presented in [21] is the following:

$$\lambda(dv) = \int_{dm}\int_{edp}\int_{im} G(dv \mid dm)dG(dm \mid edp)dG(edp \mid im)d\lambda(im) \tag{1}$$

where *im*, *edp*, *dm*, and *dv* are the intensity measure, engineering demand parameter, damage measure, and decision variable, respectively, $\lambda(x)$ is the mean annual rate of events exceeding a given level for a given variable x, $G(x)$ is the complementary cumulative distribution function (CCDF) for random variable X, i.e., $G(x) = \Pr(X > x)$, and the corresponding conditional CCDF $G(x \mid y) = \Pr(X > x \mid Y = y)$. Moreover, the variables *im*, *edp*, and *dm* can be expressed in vector form, i.e., multiple folds are implied in the integrals.

In this study, a reference benchmark *PDSD* is developed based on the PEER PBEE framework considering the first two sources of uncertainties, i.e., the earthquake intensity measure and the structural response of a certain damage group corresponding to a group of structural components affected by the same *EDP* [13], in the investigated RC highway bridge structures. In addition, this study is extended to account for structural collapse. Eq. (2) presents the general formula for the *PDSD* as follows:

$$G(edp) = \Pr(EDP > edp) = \int_{\boldsymbol{im}} G(edp \mid \boldsymbol{im}) f_{\mathbf{IM}}(\boldsymbol{im}) d\boldsymbol{im} \tag{2}$$

where $\boldsymbol{im} = (im_1, im_2, \ldots, im_{n_{im}})$, $\mathbf{IM} = (IM_1, IM_2, \ldots, IM_{n_{im}})$, n_{im} is the number of intensity measures considered, $\int_{\boldsymbol{im}}(\cdot)d\boldsymbol{im}$ is an abbreviated form of $\int_{im_1}\int_{im_2}\cdots\int_{im_{n_{im}}}(\cdot)dim_1 dim_2 \cdots dim_{n_{im}}$, $G(edp \mid \boldsymbol{im}) = \Pr(EDP > edp \mid \mathbf{IM} = \boldsymbol{im})$

is the conditional probability of *EDP* exceeding the seismic demand level *edp* given the intensity measures $\boldsymbol{im}$, and $f_{\mathbf{IM}}(\boldsymbol{im})$ is the joint probability density function (PDF) of the intensity measures.

4.1 Ground motion selection for the benchmark *PDSD*

The reference benchmark *PDSD* is developed from a large amount of NTHA simulations. The GM records for these simulations are selected based on the procedures in [22, 23] yielding a total of 600 pairs of bidirectional horizontal GMs for each bridge of each abutment modeling.

For evaluating the *PDSD* estimates from different GMSM procedures, four *EDP*s are selected, namely the peak abutment unseating displacement, column drift ratio, column base shear, and column top curvature. Moreover, different intercept angles, varying from 0° to 150° with an increment of 30°, are investigated. Therefore, considering the three RC highway bridges A, B, and C, two abutment analytical modeling types I and II, and the above-mentioned six intercept angles, $600\times3\times2\times6$=21,600 NTHA simulations [24] are performed in total for the determination of the reference benchmark *PDSD*.

4.2 Intensity measures

Many research efforts were devoted to the intensity measures (e.g., [25]). Various studies have shown that *PGV* can be considered as a reasonable GM intensity measure that correlates well with the peak nonlinear oscillator response (e.g., [26]). In this study, the natural logarithm of *PGV*s of two directions of GM records are selected as the intensity measures, i.e., $\mathbf{IM}=[\ln(PGV_1)\quad \ln(PGV_2)]$, to account for the distinct behaviors in the longitudinal and transverse directions of the considered bridge structures. Therefore, $f_{\mathbf{IM}}(\boldsymbol{im})$ in Eq. (2) becomes the joint PDF of $\ln(PGV_1)$ and $\ln(PGV_2)$. A non-parametric statistical inference, multivariate kernel density estimation [27, 28] is applied to estimate $f_{\mathbf{IM}}(\boldsymbol{im})$ for the investigated three RC highway bridges, refer to Figure 3 as an example.

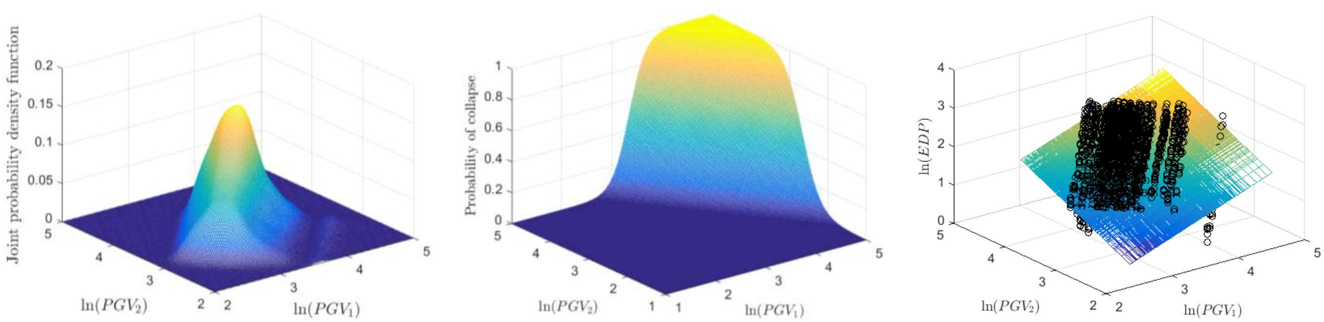

a) Joint PDF b) Fragility surface c) Linear regression surface

Figure 3. Joint PDF, fragility surface and linear regression surface of column drift for bridge B (Type I abutment model) with $\overline{DR}=8\%$.

4.3 Collapse consideration

When developing the *PDSD* of the investigated bridges, it is necessary to account for the possibility that some GM records, whose $\mathbf{IM}$ are at high levels, may cause collapse of the bridge. From Eq. (2), the probability that $edp\,|\,\boldsymbol{im}$ is exceeded is investigated by the summation of probabilities of such occurrences conditioned on the two mutually exclusive categories of the bridge collapse (C) and non-collapse (NC), i.e.,

$$G(edp\,|\,\boldsymbol{im})=G(edp\,|\,\boldsymbol{im},\mathrm{C})\times\Pr(\mathrm{C}\,|\,\boldsymbol{im})+G(edp\,|\,\boldsymbol{im},\mathrm{NC})\times\Pr(\mathrm{NC}\,|\,\boldsymbol{im}) \tag{3}$$

Assuming that $G(edp \mid \boldsymbol{im}, \mathrm{C}) = 1.0$, Eq. (3) leads to the following:

$$G(edp \mid \boldsymbol{im}) = \Pr(\mathrm{C} \mid \boldsymbol{im}) + G(edp \mid \boldsymbol{im}, \mathrm{NC}) \times [1 - \Pr(\mathrm{C} \mid \boldsymbol{im})] \tag{4}$$

In this study, two failure criteria are defined: (1) deck unseating, and (2) column excessive rotation; whichever takes place first. Deck unseating is assumed to occur when the abutment unseating displacement is larger than the length of the abutment seat, which is taken as 33.85 inches. The limit state corresponding to the column excessive rotation is defined as exceeding certain threshold of the column drift ratio ($\overline{DR}$).

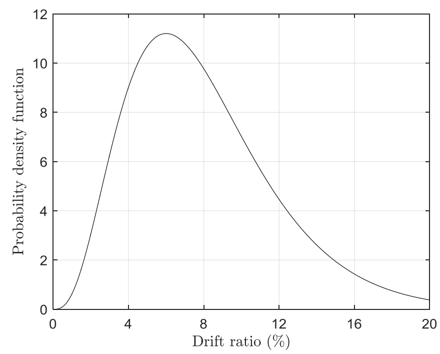

Figure 4. Assumed gamma distribution of $\overline{DR}$.

Hutchinson et al. [29] demonstrated that, on the basis of the mean trend from their experimental data, if the maximum drift ratios are less than about 8%, the residual drift ratios are generally less than 1%, which is the allowable residual drift ratio suggested in [30]. The maximum drift ratios of about 6% were recommended in [29] if a higher degree of confidence is required. In this study, $\overline{DR}$ is assumed to have a gamma distribution (Figure 4) with mean and mode equal to 8% and 6%, respectively. From the prescribed collapse criteria, Eq. (4) is further manipulated as follows:

$$G(edp \mid \boldsymbol{im}) = \int_{\overline{dr}} \{\Pr(\mathrm{C} \mid \boldsymbol{im}) + G(edp \mid \boldsymbol{im}, \mathrm{NC}) \times [1 - \Pr(\mathrm{C} \mid \boldsymbol{im})]\} f_{\overline{DR}}(\overline{dr}) d\overline{dr} \tag{5}$$

where $f_{\overline{DR}}(\overline{dr})$ is the PDF of the $\overline{DR}$ defined in Figure 4. The fragility surface or conditional probability of collapse, i.e., $\Pr(\mathrm{C} \mid \boldsymbol{im})$, is evaluated using the multivariate binary logistic regression [31] by fitting a binomial distribution to the observed collapsed (1: C; 0: NC) versus $\mathbf{IM}$. Figure 3b presents $\hat{\Pr}(\mathrm{C} \mid \boldsymbol{im})$ for bridge B with Type I abutment model when $\overline{DR}$ equals 8%, i.e., the mean of the gamma distribution in Figure 4.

4.4 Non-collapse structural responses

In Eq. (5), the only term that has not been determined is the probability of *EDP* exceeding the seismic demand level *edp* given the intensity measures for the non-collapse scenario, i.e., $G(edp \mid \boldsymbol{im}, \mathrm{NC})$. In this study, the distribution of *EDP*s conditioned on the intensity measures, i.e., $\ln(PGV_1)$ and $\ln(PGV_2)$, is assumed to be lognormal (e.g., [32]). Multivariate linear regression [31] is used to estimate this distribution. Figure 3c illustrates the linear regression surface of the column drift for bridge B with Type I abutment model when $\overline{DR}$ equals 8%.

4.5 Integration of intensity measures and structural responses

Combination of intensity measures from the kernel density estimator and structural responses, including C and NC cases, i.e., substituting Eq. (5) and their estimates into Eq. (2), leads to

$$\hat{G}(edp) = \int_{\boldsymbol{im}}\int_{\overline{dr}} \left\{ \hat{\Pr}(\mathrm{C} \mid \boldsymbol{im}) + \hat{G}(edp \mid \boldsymbol{im}, \mathrm{NC}) \times \left[1 - \hat{\Pr}(\mathrm{C} \mid \boldsymbol{im})\right] \right\} \hat{f}_{\overline{DR}}(\overline{dr}) \hat{f}_{\mathbf{IM}}(\boldsymbol{im})\, d\overline{dr}\, d\boldsymbol{im} \tag{6}$$

In general, it is impossible to determine the exact solution of the integrations in Eq. (6). Instead, in practice, $\hat{G}(edp)$ in Eq. (6) is computed from the following discretized form:

$$\hat{G}(edp) \cong \sum_k \sum_j \sum_i \left\{ \hat{\Pr}(\mathrm{C}_i \mid \boldsymbol{im}_{jk}) + \hat{G}(edp \mid \boldsymbol{im}_{jk}, \mathrm{NC}_i) \times \left[1 - \hat{\Pr}(\mathrm{C}_i \mid \boldsymbol{im}_{jk})\right] \right\} \hat{\Pr}(\overline{dr}_i) \hat{\Pr}(\boldsymbol{im}_{jk}) \tag{7}$$

where $\hat{\Pr}(\mathrm{C}_i \mid \boldsymbol{im}_{jk})$ and $\hat{G}(edp \mid \boldsymbol{im}_{jk}, \mathrm{NC}_i)$ are respectively the estimated probabilities of collapse and exceedance in the context of NC, when $dr = \overline{dr}_i$, conditioning on $\mathbf{IM} = \boldsymbol{im}_{jk}$, i.e., $\ln(PGV_1) = \ln(pgv_1^j)$ and $\ln(PGV_2) = \ln(pgv_2^k)$.

Comparing Eq. (7) with Eq. (6), the integrals, the PDF, and the joint PDF are replaced with the summations, the probability mass function (PMF), and the joint PMF, respectively. The symbol "$\cong$" in Eq. (7) signifies the approximation due to the discretization of the continuous integral of the seismic demand. It should be noted that this study aims at evaluating GMSM procedures in the context of a given large earthquake that results in highly nonlinear responses. The procedures of the benchmark *PDSD* development, however, is readily extended to the case of multiple earthquake scenarios as follows:

$$\hat{G}_m(edp) \cong \sum_{l=1}^{N_{eqs}} \nu_l \cdot \left\{ \sum_k \sum_j \sum_i \left\{ \hat{\Pr}(\mathrm{C}_i \mid \boldsymbol{im}_{jk}) + \hat{G}(edp \mid \boldsymbol{im}_{jk}, \mathrm{NC}_i) \times \left[1 - \hat{\Pr}(\mathrm{C}_i \mid \boldsymbol{im}_{jk})\right] \right\} \hat{\Pr}(\overline{dr}_i) \hat{\Pr}(\boldsymbol{im}_{jk}) \right\}_l \tag{8}$$

where $\hat{G}_m(edp)$ is the *PDSD* for multiple earthquake scenarios with number N_{eqs} and ν_l is the activity rate [25] for the *l*-th earthquake scenario.

5. Evaluation of the GMSM Procedures

Three GMSM procedures from the two categories mentioned previously are investigated in this study. The first amplitude scaling procedure is the conventional first mode spectral acceleration, i.e., $S_a(T_1)$, selection and scaling method. The other two, namely the conditional mean spectrum (*CMS*) and the unconditional selection (*US*) methods, are spectrum shape matching procedures. They match the CMS and the median $+1.5\varepsilon$ spectrum in Figure 2, respectively. Detailed descriptions of these three methods and their selection procedures can be found in [22, 23, 33].

For each bridge with each abutment modeling, 40 GM records are selected for each investigated GMSM procedure, including two versions of $S_a(T_1)$, namely $S_a(T_1)$ and $S_a(T_1)_p$ scaling and selection method[1*], i.e., a total of four GMSM procedures. Similar to the development of the reference benchmark *PDSD*, these GMs are applied to each bridge with six different intercept angles. Thus, besides 21,600 NTHA simulations for the development of the benchmark *PDSD*, 40×4×3×2×6=5,760 more NTHA analyses are performed for all the GMSM procedures.

The *PDSD* estimates by the 40 GM records from each GMSM investigated procedures are compared against the benchmark *PDSD* to evaluate their accuracy and reliability. Analogous to Eqs. (3) and (4), $G(edp)$ is divided into two mutually exclusive categories of C and NC, i.e.,

$$\begin{aligned} G(edp) &= G(edp \mid \mathrm{C}) \times \Pr(\mathrm{C}) + G(edp \mid \mathrm{NC}) \times \Pr(\mathrm{NC}) \\ &= \Pr(\mathrm{C}) + G(edp \mid \mathrm{NC}) \times \left[1 - \Pr(\mathrm{C})\right] \end{aligned} \tag{9}$$

[*]Comparing to the traditional $S_a(T_1)$ method, $S_a(T_1)_p$ method considers the contribution of pulse-like GM based on [34].

where it is assumed that $G(edp \mid \mathrm{C}) = 1.0$ and $\Pr(\mathrm{C})$ is the probability of collapse estimated as:

$$\hat{\Pr}(\mathrm{C}) = \frac{\#\text{ of records causing collapse}}{\text{total}\#\text{ of records} = 40} \tag{10}$$

The probability of exceedance for the NC cases, i.e., $G(edp \mid \mathrm{NC})$, can be estimated by a nonparametric inference using the following empirical CCDF (e.g., [35]):

$$\hat{G}(edp \mid \mathrm{NC}) = \frac{1}{m}\sum_{l=1}^{m} I\left(EDP_l > edp\right) \tag{11}$$

where m is the number of GM records that produce NC, EDP_l is the value of *EDP* for the *l*-th record, and $I(\cdot)$ represents the indicator function (i.e., $I(EDP_l > edp) = 1.0$ if $EDP_l > edp$; otherwise, $I(EDP_l > edp) = 0.0$). Recall the previously discussed collapse criterion, along with the estimates in Eqs. (10) and (11), the *PDSD* estimate, i.e., $\hat{G}(edp)$, is obtained as follows:

$$\hat{G}(edp) = \int_{\overline{dr}} \left\{\hat{\Pr}(\mathrm{C}) + \hat{G}(edp \mid \mathrm{NC}) \times \left[1 - \hat{\Pr}(\mathrm{C})\right]\right\} \hat{f}_{\overline{DR}}\left(\overline{dr}\right) d\overline{dr} \tag{12}$$

Following similar procedure from Eq. (6) and Eq. (7), $\hat{G}(edp)$ in Eq. (12) is computed from the following discretized form:

$$\hat{G}(edp) \cong \sum_{i} \{\hat{\Pr}(\mathrm{C}_i) + \hat{G}(edp \mid \mathrm{NC}_i) \times [1 - \hat{\Pr}(\mathrm{C}_i)]\} \hat{\Pr}\left(\overline{dr}_i\right) \tag{13}$$

where $\hat{\Pr}(\mathrm{C}_i)$ and $\hat{G}(edp \mid \mathrm{NC}_i)$ are respectively the estimated probabilities of collapse and exceedance in the NC cases when $dr = \overline{dr}_i$. Figures 5-7 present the comparison of the *PDSD* estimates of six different intercept angles from the four investigated GMSM procedures and the benchmark *PDSD*. Such comparisons are given for the peak column shear force for bridges A (Type II abutment modeling) (Figure 5), the peak unseating displacement for bridges B (Type I abutment modeling) (Figure 6), and the peak column drift ratio for bridges C (Type I abutment modeling) (Figure 7). All other results are given in [22, 23].

It is observed from Figure 5 that the *PDSD* estimates from the $S_a(T_1)$ and $S_a(T_1)_p$ procedures generally underestimate the seismic demands from the benchmark *PDSD* for bridge A. In general, e.g., from Figures 5 and 6, the *PDSD* estimates from the $S_a(T_1)_p$ procedure are larger and more accurate than the ones estimated from the $S_a(T_1)$ procedure. Such observations are attributed to the fact that more pulse motions that result in large responses are selected in the $S_a(T_1)_p$ procedure. From Figures 5 and 6, the *PDSD* estimates from the *CMS* method almost always underestimate the seismic demands, especially for the large values of *EDP*s (the tail of the *PDSD* curve), for bridges A and B. In contrast, the *PDSD* estimates by the *US* method are almost always on the conservative side with approximately 10%~20% overestimation of the probability of exceedance over the benchmark *PDSD*. For bridge C, as shown in Figure 7, all four GMSM procedures overestimate the seismic demands.

Based on the simulation results, the estimates by the *US* procedure are almost always on the conservative side and are usually the most conservative of all GMSM procedures for all three bridges. The $S_a(T_1)$ and $S_a(T_1)_p$ procedures show some superiority over the *CMS* method (e.g., in predicting *PDSD* for bridges A and B); while they sometimes underestimate the responses, e.g., in bridge A. As discussed previously, RC highway bridges play a crucial role in transportation and thus require short downtime after severe earthquakes from an emergency response and, more generally, community resiliency points of view. Therefore, among these four investigated GMSM procedures, it is suggested to use the *US* method for selection and modification of GMs.

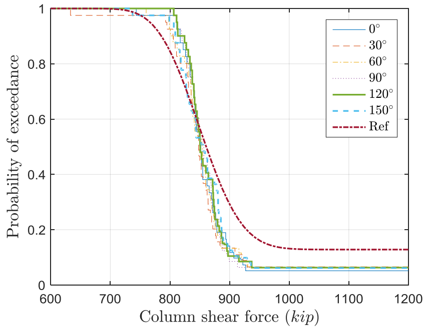

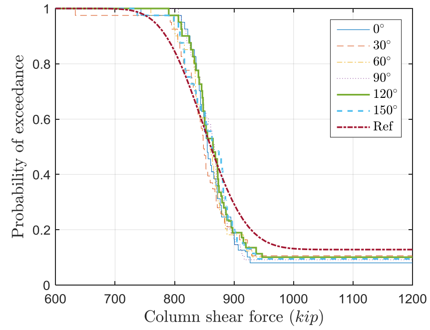

a) $S_a(T_1)$ b) $S_a(T_1)_p$

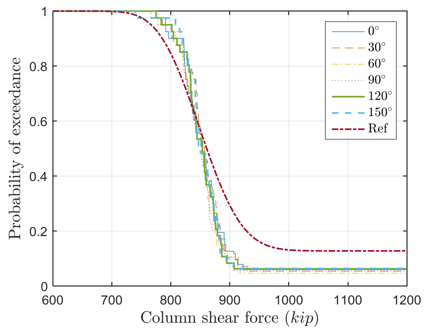

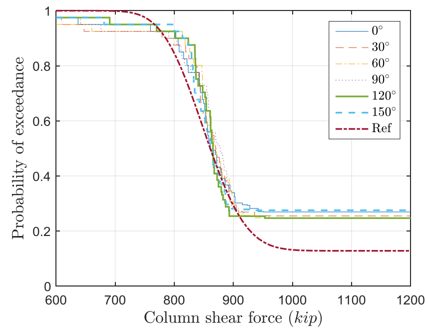

c) *CMS* d) *US*

Figure 5. *PDSD* estimates of peak shear force of different intercept angles from four GMSM procedures for bridge A with Type II abutment modeling.

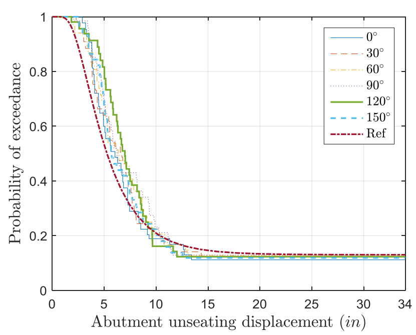

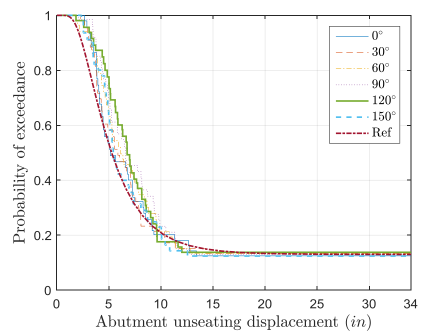

a) $S_a(T_1)$ b) $S_a(T_1)_p$

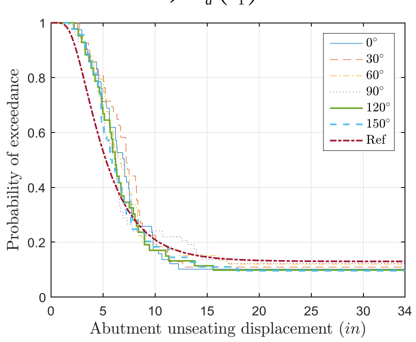

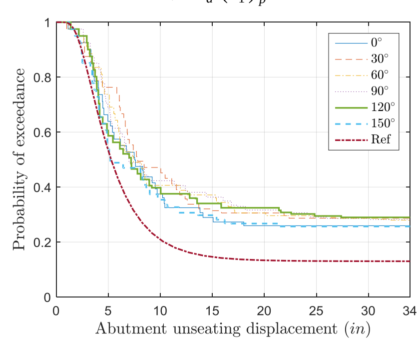

c) *CMS* d) *US*

Figure 6. *PDSD* estimates of peak unseating displacement of different intercept angles from four GMSM procedures for bridge B with Type I abutment modeling.

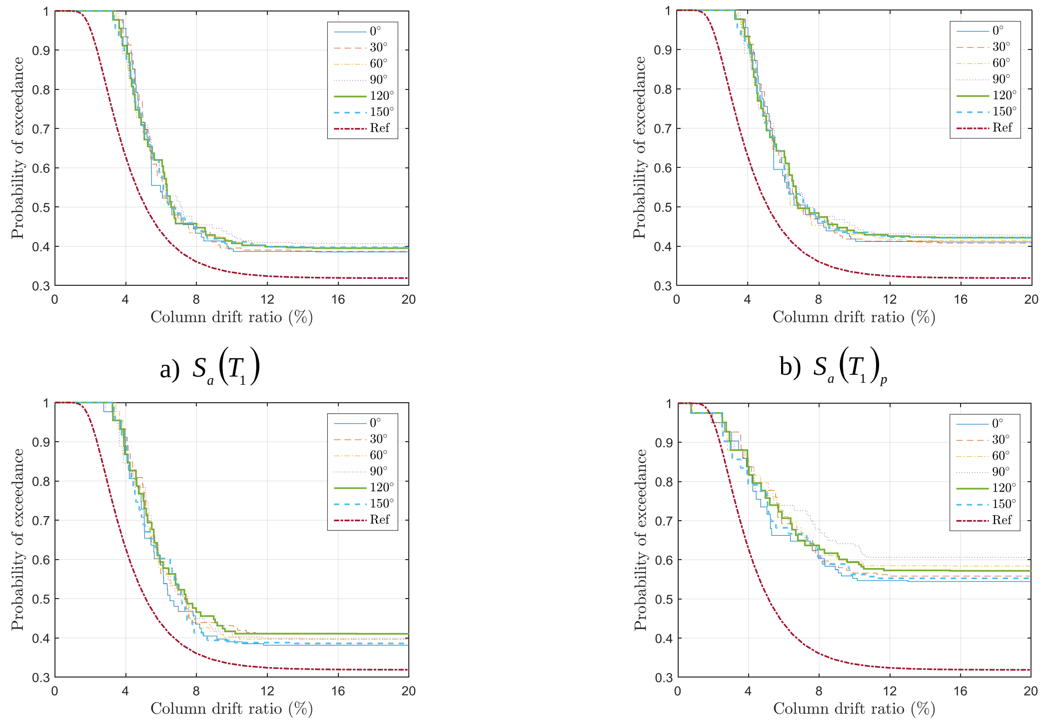

a) $S_a(T_1)$ b) $S_a(T_1)_p$

c) *CMS* d) *US*

Figure 7. *PDSD* estimates of column drift ratio of different intercept angles from four GMSM procedures for bridge C with Type I abutment modeling.

7. Conclusions

This study evaluates several GMSM procedures in predicting the *PDSD* of RC highway bridges subjected to large earthquakes that result in highly nonlinear responses. Taking advantage of the PEER PBEE methodology, this paper develops the benchmark *PDSD* by taking into account the uncertainties of earthquake intensity measures and structural responses. The accuracy and reliability of all the *PDSD* estimates from the investigated GMSM procedures are evaluated against the reference benchmark *PDSD*. Such evaluations are conducted on four selected *EDP*s of three representative RC highway bridges with two types of abutment modeling. In total, 27,360 NTHA simulations, where 21,600 ones for the development of the benchmark *PDSD* and 5,760 ones for the *PDSD* estimates by the GMSM procedures, are performed in this study. Major findings are summarized as follows:

1. Two intensity measures are selected to account for distinct behaviors in longitudinal and transverse directions of the bridge structures. A non-parametric inference, multivariate kernel density estimation, is utilized to estimate the joint PDF of the two intensity measures.
2. The structural collapse scenario, including the uncertainty of the collapse criteria, is considered and incorporated into the *PDSD* estimate. The conditional probability of collapse and that of *EDP*s are respectively estimated by multivariate binary logistic and linear regressions.
3. The procedures of the benchmark *PDSD* development in the context of a large given earthquake scenario can be readily extended to the case of multiple earthquake scenarios. Future investigation will focus on simulations considering such multiple scenarios.
4. In general, the *PDSD* estimates from the $S_a(T_1)_p$ procedure are larger and more accurate than the ones estimated from the $S_a(T_1)$ procedure. The $S_a(T_1)$ and $S_a(T_1)_p$ procedures present certain superiority over the *CMS* method while all three procedures underestimate the seismic demands for some bridges.
5. The *PDSD* estimates by the *US* procedure are almost always on the conservative side and accordingly the

most conservative of all investigated GMSM procedures. The RC highway bridges are essential lifeline infrastructures in transportation and thus their possible long downtime after severe earthquakes is not affordable for both the emergency response and community resiliency aspects. Thus, among all four investigated GMSM procedures, it is recommended to use the *US* for selection and modification of GMs.

7. Acknowledgement

Prof. Farzin Zareian, University of California, Irvine, is acknowledged for providing the OpenSees models of the analyzed bridges. This research was supported by Caltrans (Contract # 65A0454) for the project "Guidelines for nonlinear seismic analysis of ordinary bridges." The authors thank Caltrans for this support.

8. References

[1] Benzoti, G., Ohtaki, T., Pristley, M. J. N., Seible, F. (1996): Seismic performance of circular reinforced concrete columns under varying axial load, Division of Structural Engineering, 96/04, University of California, San Diego, CA.

[2] Liang X, Mosalam KM, Günay S (2016): Direct Integration Algorithms for Efficient Nonlinear Seismic Response of Reinforced Concrete Highway Bridges. *ASCE Journal of Bridge Engineering*, 21(7), 04016041.

[3] Mosalam KM, Liang X, Günay S, Schellenberg A (2013): Alternative Integrators and Parallel Computing for Efficient Nonlinear Response History Analyses. *4th International Conference on Computational Methods in Structural Dynamics and Earthquake Engineering (COMPDYN)*, Kos Island, Greece.

[4] Shome N, Cornell CA, Bazzurro P, Carballo, JE (1998): Earthquakes, records, and nonlinear response. *Earthquake Spectra*, **14**(3), 469-500.

[5] Tothong P, Luco N (2007): Probabilistic seismic demand analysis using advanced ground motion intensity measures," *Earthquake Engineering & Structural Dynamics*, **36**(13), 1837-1860.

[6] Luco N, Cornell CA (2007): Structure-specific scalar intensity measures for near-source and ordinary earthquake ground motions. *Earthquake Spectra*, **23**(2), 357-392.

[7] Kottke A, Rathje EM (2008): A semi-automated procedure for selecting and scaling recorded earthquake motions for dynamic analysis. *Earthquake Spectra*, **24**(4), 911-932.

[8] Baker JW (2011): Conditional mean spectrum: Tool for ground-motion selection. *ASCE Journal of Structural Engineering*, **137**(3), 322-331.

[9] Katsanos EI, Sextos AG, Manolis GD (2010): Selection of earthquake ground motion records: A state-of-the-art review from a structural engineering perspective. *Soil Dynamics & Earthquake Engineering*, **30**(4), 157–169.

[10] Haselton CB, Baker JW, Bozorgnia Y, Goulet CA, Kalkan E, Luco N, Shantz TJ, Shome N, Stewart JP, Tothong P, Watson-Lamprey JA, Zareian F (2009): Evaluation of Ground Motion Selection and Modification Methods: Predicting Median Interstory Drift Response of Buildings. *Technical Report PEER 2009/01*, Pacific Earthquake Engineering Research, Berkeley, USA.

[11] Hancock J, Bommer JJ, Stafford PJ (2008): Numbers of scaled and matched accelerograms required for inelastic dynamic analyses. *Earthquake Engineering & Structural Dynamics*, **37**(14), 1585-1607.

[12] Heo Y, Kunnath SK, Abrahamson N (2010): Amplitude-scaled versus spectrum-matched ground motions for seismic performance assessment. *ASCE Journal of Structural Engineering*, **137**(3), 278-288.

[13] Günay S, Mosalam KM (2013): PEER performance-based earthquake engineering methodology, revisited. *Journal of Earthquake Engineering*, **17**(6), 829-858.

[14] Kaviani P, Zareian F, Taciroglu E (2014): Performance-Based Seismic Assessment of Skewed Bridges, *Technical Report PEER 2014/01*, Pacific Earthquake Engineering Research, Berkeley, USA.

[15] Kaviani P, Zareian F, Taciroglu E (2012): Seismic Behavior of Reinforced Concrete Bridges with Skew-Angled Seat-Type Abutments. *Engineering Structure*, **45**, 137-150.

[16] McKenna F, Fenves GL, Filippou FC (2010): The Open System for Earthquake Engineering Simulation, Pacific Earthquake Engineering Research, Berkeley, USA.

[17] Aviram A, Mackie KR, Stojadinović B (2008): Guidelines for Nonlinear Analysis of Bridge Structures in California, *Technical Report PEER 2008/03*, Pacific Earthquake Engineering Research, Berkeley, USA.

[18] Omrani R, Mobasher B, Liang X, Günay S, Mosalam KM, Zareian F, Taciroglu E (2015): Guidelines for Nonlinear Seismic Analysis of Ordinary Bridges: Version 2.0, *Technical Report CA 15-2266*, California Department of Transportation, Sacramento, USA.

[19] Campbell KW, Bozorgnia Y (2008): NGA Ground Motion Model for the Geometric Mean Horizontal Component of PGA, PGV, PGD and 5% Damped Linear Elastic Response Spectra for Periods Ranging from 0.01 to 10s. *Earthquake Spectra*, **24**(1), 139–171.

[20] Moehle JP, Deierlein GG (2004): A Framework Methodology for Performance-based Earthquake Engineering. *13th International World Conference on Earthquake Engineering (13WCEE)*, Vancouver, Canada.

[21] Cornell CA, Krawinkler H (2000): Progress and challenges in seismic performance assessment. *PEER Center News*, **3**(2), 1-3.

[22] Liang X, Mosalam KM (2016): Probabilistic Evaluation of Ground Motion Selection and Modification Procedures for Reinforced Concrete Highway Bridges. *Earthquake Engineering & Structural Dynamics* (under review).

[23] Liang X (2016): Performance-Based Robust Nonlinear Seismic Analysis with Application to Reinforced Concrete Bridge Systems. *Ph.D. Dissertation*, University of California, Berkeley, USA.

[24] Liang X, Günay S, Mosalam KM (2016): Integrators for Nonlinear Response History Analysis: Revisited. *Istanbul Bridge Conference*, Istanbul, Turkey.

[25] Bradley BA (2013): A comparison of intensity-based demand distributions and the seismic demand hazard for seismic performance assessment. *Earthquake Engineering & Structural Dynamics*, **42**(15), 2235-2253.

[26] Riddell R (2007): On ground motion intensity indices. *Earthquake Spectra*, **23**(1), 147-173.

[27] Härdle W, Muller M, Sperlich S, Werwatz A (2004): *Nonparametric and Semiparametric Models: An Introduction*, Springer.

[28] Botev ZI, Grotowaski JF, Kroese DP (2010): Kernel density estimation via diffusion. *The Annals of Statistics*, **38**(5), 2916-2957.

[29] Hutchinson TC, Chai YH, Boulanger RW (2004): Inelastic seismic response of extended pile-shaft-supported bridge structures. *Earthquake Spectra*, **20**(4), 1057-1080.

[30] MacRae GA, Kawashima K (1997): Post-earthquake Residual Displacements of Bilinear Oscillators. *Earthquake Engineering & Structural Dynamics*, **26**(7), 701-716.

[31] Wasserman L (2010): *All of statistics: A concise course in statistical inference*, Springer, 3rd edition.

[32] Kunnath SK, Larson L, Miranda E (2006): Modeling considerations in probabilistic performance-based seismic evaluation: Case study of the I-880 viaduct. *Earthquake Engineering& Structural Dynamic*, **35**(1), 57-75.

[33] Liang, X, Günay, S, Mosalam, KM (2016). *Chapter 12: Seismic Response of Bridges Considering Different Ground Motion Selection Methods*, in *Developments in International Bridge Engineering*, Springer Tracts on Transportation and Traffic 9, Springer Int. Publishing, Switzerland.

[34] Hayden C, Bray J, Abrahamson N, Acevedo-Cabrera AL (2012): Selection of Near-Fault Pulse Motions for Use in Design. *15th International World Conference on Earthquake Engineering (15WCEE)*, Lisbon, Portugal.

[35] Baker JW (2007): Probabilistic structural response assessment using vector-valued intensity measures. *Earthquake Engineering & Structural Dynamics*, **36**(13), 1861-1883.